The Pitching Delta Wing

Mohamed Gad-el-Hak* and Chih-Ming Ho†
Flow Research Company, Kent, Washington

Delta wings in steady flow can provide high lift at large angles of attack and are therefore used on many high-performance aircrafts. However, the unsteady aerodynamic properties of a delta wing are practically unknown, although vital for operating and designing airplanes for poststall and other maneuvering. In this study, the flowfields around two pitching delta wings with apex angles of 90 and 60 deg were visualized in a towing tank at chord Reynolds numbers up to 3.5×10^5. The reduced frequency was varied in the range 0.05-3. The leading-edge separation vortex went through a growth-decay cycle with hysteresis during a pitching period. A distinct change of the separated flow was observed at a reduced frequency around π.

Nomenclature

$\mathcal{R}$	= aspect ratio
c	= root chord
f	= pitching frequency
H	= height of the dyed region in $y-z$ plane
K	= reduced frequency, $=\pi fc/U_\infty$
N	= Brunt-Väisälä frequency
R_c	= chord Reynolds number, $=U_\infty c/\nu$
s	= wing semispan
t	= time, s
U_∞	= towing speed
V	= vertical velocity
V_w	= vertical velocity at the wing surface
x,y,z	= Cartesian coordinates fixed with the wing
$\alpha(t)$	= angle of attack
α_0	= mean angle of attack
β	= apex angle
γ	= angle between vortex cores
λ	= perturbation wavelength
ν	= kinematic viscosity

I. Introduction

In a steady flow, the lift of a two-dimensional airfoil is contributed mainly by the leading-edge suction peak. The lift increases with increasing angle of attack until the stall angle is reached. The separation on the upper surface will then reduce the leading-edge suction peak causing the lift to drop. The static stall angle for a two-dimensional airfoil is about 12 deg. The lift-producing mechanism of a delta wing is somewhat different. The leading-edge suction peaks predicted by potential theory do not exist.[1] Instead, two smooth suction peaks inward of the leading edges are detected. These peaks are produced by a pair of stationary leading-edge vortices formed by separated flow on the low-pressure side of the wing. Therefore, the lift on a delta wing is created by the *separated* vortical structures rather than by the attached flow over a convex surface. The lift keeps increasing with α until the leading-edge vortex breaks down at an angle of attack of 30 deg or more. Hence, a delta wing is a good means to obtain high lift at large angles of attack. The aspect ratio of a delta wing is relatively small, which results in a low lift-to-drag ratio at subsonic speeds. Accordingly, delta wings are designed primarily for supersonic speeds.

Fairly extensive studies about the steady flow around delta wings have been reported by various researchers. The flowfield is determined essentially by the sweep angle of the leading edge, the cross sectional shape, and the angle of attack. Elle[2] examined the core positions of the separation vortex as a function of the angle of attack. He visualized the vortices by using air bubbles in a water channel. The angle between the two cores, γ, does not change significantly at different angles of attack. The ratio between γ and the apex angle β stays around 0.6, but the vortex cores lift away from the wing surface with increasing α. Fink and Taylor[3] investigated the pressure distribution on a wing with $\beta=20$ deg. The suction peaks of the spanwise pressure distribution at several chordwise locations always occurred at about 60% of the semispan from the center for all tested angles of attack, 5 deg $\leq\alpha\leq$ 30 deg. In other words, the suction peaks were located under the vortex cores.

Under practical conditions, fast maneuvering is always required for high-performance airplanes. The unsteady aerodynamic properties can be significantly different from those in steady flow. The operation of the aircraft can either benefit or be hampered by the special features in the unsteady flow. For example, the maximum lift of a pitching two-dimensional airfoil is much higher than the static maximum lift.[4,5] However, the dynamic stall is much more abrupt than the static stall. In the case of a delta wing, the pressing problem is that the unsteady aerodynamic properties are practically unknown,[5,6] although the delta wing is the main type of airfoil used on high-performance airplanes.

In the present investigation, the unsteady flowfield around a delta wing was visualized by several dye techniques. The experimental approach is discussed in Sec. II. The detailed development process of the leading-edge separation vortex is first described in Sec. III. Then, the hysteresis loop of the vortex, the effect of the reduced frequency, as well as the existence and possible importance of a counterrotating vortex are discussed.

II. Experimental Approach

Model and Test Conditions

Two delta wings with leading-edge sweeps of 45 and 60 deg were used in the present investigation. The root chord of both wings was 25 cm, and the chord Reynolds number varied in the range of 2.5×10^4 to 3.5×10^5. Figure 1 is a sketch of the 45-deg delta wing, which had an NACA 0012 profile at each

Received Aug. 10, 1984; revision received Dec. 4, 1984.

*Senior Research Scientist. Member AIAA.

†Consultant. Permanent address: Department of Aerospace Engineering, University of Southern California, Los Angeles, CA. Member AIAA.

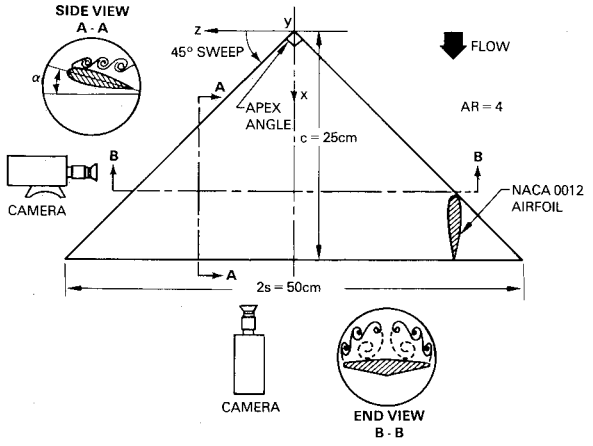

Fig. 1 Schematic of the delta wing and definition sketch.

spanwise section. The wing was made of two aluminum pieces with grooves on the inner surface of each for dye passage and storage. The 60-deg delta wing had a flat surface, a sharp leading edge, and was made of Plexiglas.

A four-bar mechanism was used to sting-mount and pitch the delta wing around the desired position along the chord. In the experiments reported herein, the wing was pitched around the quarter-chord position. The mean angle of attack could be set from 0 to 45 deg. A Boston Ratiotrol motor drove the four-bar linkages to produce approximately sinusoidal oscillations of amplitudes ± 5, ± 10, and ± 15 deg about a given mean angle of attack. The reduced frequency, $K \equiv \pi fc/U_\infty$, was varied in the range of 0.05 to 3.‡ A digital readout displayed the instantaneous angle of attack of the wing.

Towing Tank System

The wing used in the present investigation was towed at speeds in the range of 10-140 cm/s through the water channel described by Gad-el-Hak et al.[7] The towing tank is 18 m long, 1.2 m wide, and 0.9 m deep. The pitching mechanism was rigidly mounted on a carriage that rides on two tracks mounted on top of the towing system. During towing, the carriage was supported by an oil film, which ensured a vibrationless tow. The equivalent freestream turbulence was checked using a hot-film probe, and was found to be about 0.1% of the mean towing speed.

Flow Visualization

Food color and fluorescent dyes were used in the present investigation. The food color dyes were illuminated with conventional flood lights. The fluorescent dyes were excited with sheets of laser light projected in the desired plane. To produce a sheet of light, a 5-W argon-ion laser (Spectra Physics, Model 164) was used with a mirror mounted on an optical scanner having a 720-Hz natural frequency (General Scanning, Model G124). A sine-wave signal generator, set at a frequency equal to the inverse of the camera shutter speed, drove the optical scanner to produce light sheets approximately 1-mm thick.

Side views of the flowfield were obtained using a vertical sheet of laser light in the x-y plane at $z = 10$ cm (40% of the semispan of the 45 deg sweep wing) and a camera towed with the wing but located outside the tank, as shown in Fig. 1. End views were obtained using a vertical sheet of laser light in the y-z plane at $x = 20$ cm (80% of the root chord) and an underwater camera towed behind the wing using the same carriage.

Dye sheets or dye lines were seeped into the boundary layer through a system of slots and holes on the suction side of the wing. The slots were 0.2-mm wide, milled at a 45 deg angle to minimize the flow disturbance. The holes were 0.4 mm in diameter, spaced at 1 cm center to center.

Dye was also placed in the flowfield by laying several thin, horizontal sheets prior to towing the wing. The dye layers remained thin, about 1-mm thick, due to the inhibition of vertical motion caused by introducing a weak saline stratification in the tank. The dye layers remained quiescent until disturbed by the flowfield on and around the wing. Thus, the boundary-layer flow as well as the potential flow could be observed since the dye layers existed in both flow regions. Ciné films of the runs presented in this paper are available upon request (Flow Research Films Nos. 55-59).

For the dye-layer runs, the density gradient in the tank was about 10^{-4}g/cm^4, which yields a Brunt-Väisälä frequency of $N = 0.05$ Hz. The time scale associated with this weak stratification is large compared to a typical convection time scale; hence, the stratification should have little effect on the dynamics of the flow. This was verified experimentally by conducting two runs using the dye injection method, in the presence and in the absence of stratification in the tank. The visualization patterns in the two runs were indistinguishable.

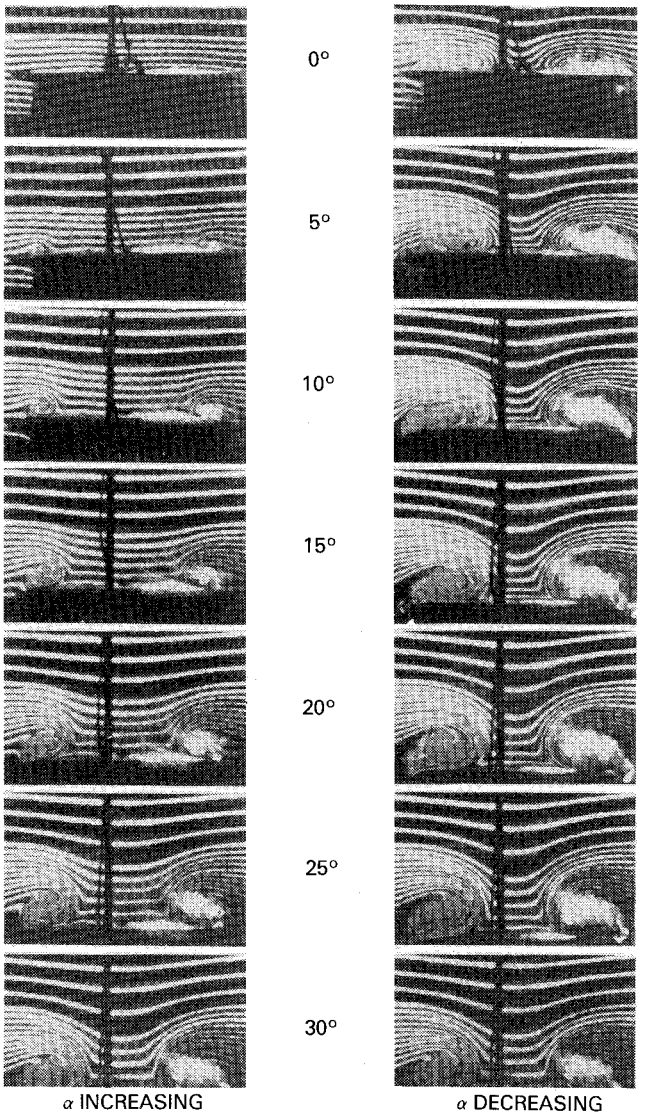

Fig. 2 End view using the dye-layer technique. $R_c = 2.5 \times 10^4$, $K = 3.0$, $\alpha^0 = 15 + 15 \sin(2.4t)$. Flow is our of the plane of the photographs.

III. Experimental Results

The main feature of the delta wing flow is the leading-edge separation vortex, which produces the lift. The flow-visualiza-

‡An aircraft will not, of course, maneuver at a reduced frequency of 3. However, several important features of the complex flowfield under investigation were more readily apparent in the high-frequency range.

tion results in the steady case are reported elsewhere.[8,9] In the unsteady case, the flow alternates between attached and separated phases during one cycle. Obviously, the complicated phenomenon of unsteady separation plays the main role in changing the aerodynamic properties.[10,11] The precise determination of the onset of the unsteady separation needs detailed surveys of the velocity and the pressure field.[12] In the present experiment, the data are obtained from visualization results, and only the first-order effect is considered here. The phase angle and the location of the separation are based upon the abrupt thickening of the dyed boundary layer.

The Overall Unsteady Flow Pattern

The complicated three-dimensional separated flow pattern of the pitching delta wing can be observed best from an overall view, which will first be discussed. Food color dyes were seeped from the slots on the suction side of the 45-deg sweep delta wing. The flowfield was illuminated with a bank of flood lights. The angle of attack was varied in the range 0-30 deg, at a reduced frequency of $K=1.0$. During the upstroke, the separation first started across the whole trailing edge at $\alpha=2$ deg (Flow Research Film 55). As the angle of attack increased, the separation vortices started to develop at the two corners of the trailing edge. The unsteady separation process looked as if a vortex sheet first peeled off from the corner of the wing and then rolled up into the separation vortex. The separation propagated from the corner toward the apex. The upstream propagation speed along the leading edge was approximately equal to the freestream speed. At $\alpha=30$ deg, the separation front reached the apex, and the separation vortices were fully developed.

During the downstroke, the flow started to reattach. Both the top view using the food color dye technique, and the end view using the dye-layer technique were used to clarify the reattachment process. As the angle of attack decreased from 30 deg, the flow near the whole leading edge (from the apex to the corners of the trailing edge) became reattached. Unlike the flow during the upstroke, there was no propagation phenomenon along the leading edge. While the angle of attack decreased, the attached area increased from the leading edge toward the centerspan. Near $\alpha=5$ deg, the flow was completely attached. Either during the separation or reattachment phase, small discrete vortices can be observed at the thin shear layer between the large separation vortex and the external potential flow.[8] This flow configuration was due to the coexistence of high-frequency instability waves and a low-frequency artificial perturbation. This phenomenon is similar to the collective interaction in an impinging jet as described by Ho and Nosseir.[13]

The dye-layer technique was used to visualize the flow near the wall as well as the external flow around the wing. When the wing passed through the quiescent dye layers, the originally flat layers were deformed. The local motion could be inferred from the moving dye layers as depicted in the movie frames. The flow was caused by the motion of the wing and the induced flow of the separation vortices. A typical case is examined here in more detail, and selected movie frames are shown in Fig. 2. The sharp-leading-edge, 60-deg delta wing underwent the pitching motion $\alpha(t)^0=15+15\sin(2.4t)$ at a chord Reynolds number of $R_c=2.5\times10^4$ and a reduced frequency of $K=3.0$. The vertical sheet of laser light was perpendicular to the flow direction and located at a chordwise location of $0.8c$. Both the upward and downward motions are shown in Fig. 2 for the attack angles of 0, 5, 10, 15, 20, 25, and 30 deg. The spanwise variations of the vertical velocity (in the laboratory frame) at $0.13c$ above the wing and at an attack angle of $\alpha=0$ deg are shown in Fig. 3. During the upstroke (the trailing edge is moving downward), the velocity near the centerspan was almost uniform and equaled about one-half of the vertical wing speed at this station. The same magnitude and a narrower region of uniform velocity were also observed during the downstroke as shown in the same figure. This result suggests that the vertical velocity near the centerspan is caused mainly by the up-down motion of the wing. The tapering of the velocity near the leading edge is due to the separation vortices.

The vertical velocities at the centerspan, along different positions above the wing, are plotted in Fig. 4 for different phase angles in a cycle. The curves were approximately sym-

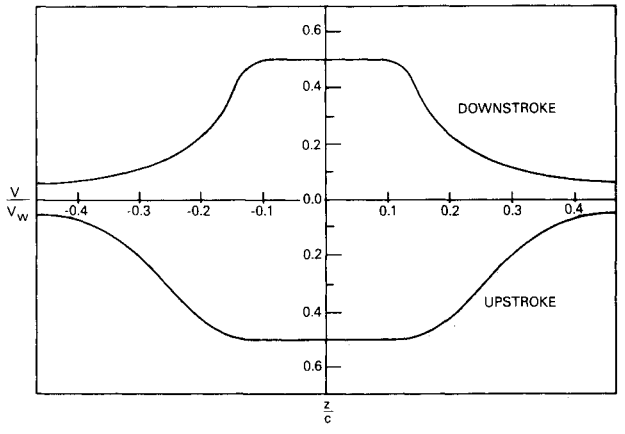

Fig. 3 Spanwise variations of vertical velocity. $R_c=2.5\times10^4$, $K=3.0$, $\alpha=0$ deg, $y/c=0.13$.

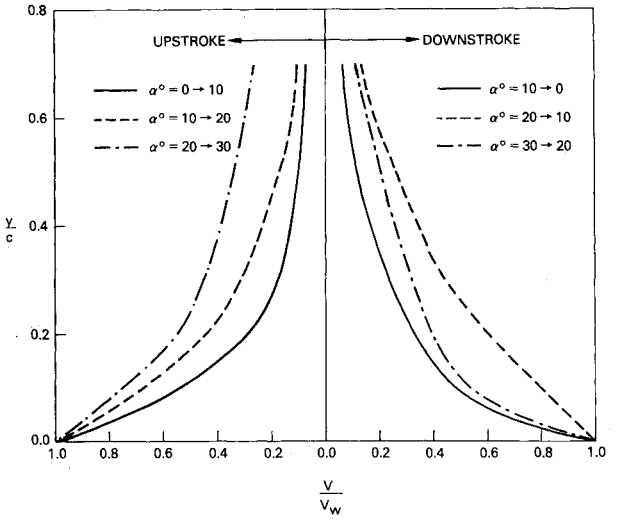

a) Linear plot.

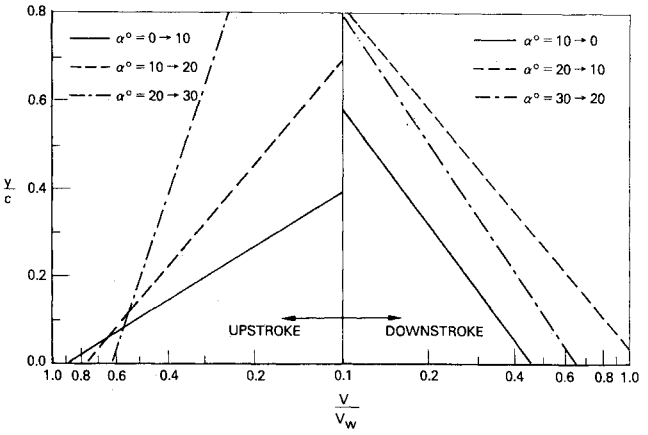

b) Semilog plot.

Fig. 4 Variations of vertical velocity with normal coordinate. $R_c=2.5\times10^4$, $K=3.0$, $\alpha^0=15\pm15$, $z/c=0$.

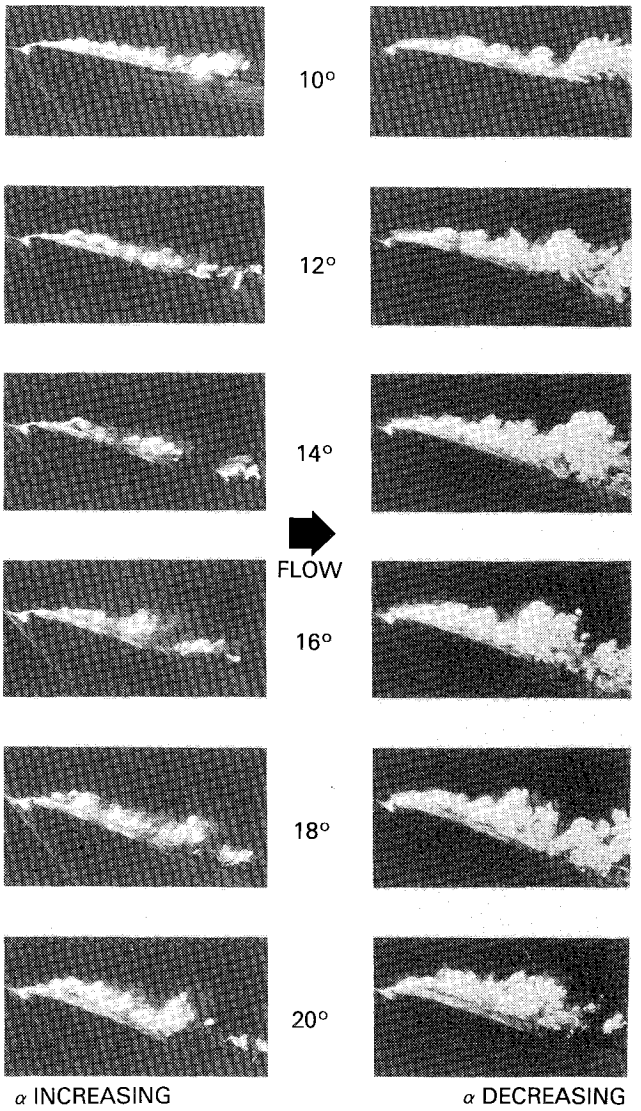

Fig. 5 Side view of pitching wing. $R_c = 2.5 \times 10^4$, $K = 0.5$, $\alpha(t)^\circ = 15 + 5 \sin(0.4t)$.

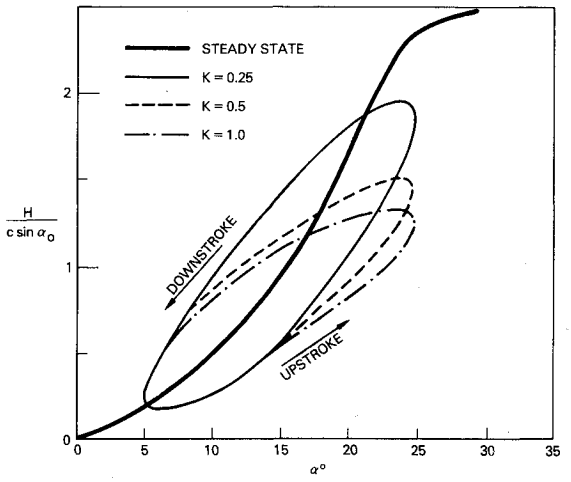

a) Effects of reduced frequency. $R_c = 5.0 \times 10^4$, $\alpha^\circ = 15 \pm 10$.

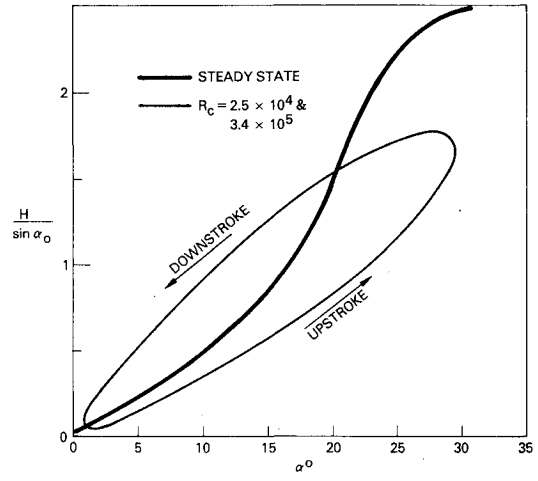

b) Effects of Reynolds number. $K = 1.0$, $\alpha^\circ = 15 \pm 15$.

Fig. 6 Hysteresis loop.

metric for corresponding phase angles during the downstroke and upstroke. The data in Fig. 4 further substantiate the aforementioned observation. Another interesting point is that the velocity decays exponentially away from the wing as shown in the semilog plot in Fig. 4b. In an incompressible flow, a large vertical gradient of the horizontal motion (streamwise or spanwise) must exist. However, measurements of the horizontal velocities were not performed in the present investigation.

The Hysteresis Loop

During one pitching cycle, the leading-edge separation vortices executed a growth-decay cycle. Figure 5 is a side view of the flow on the suction side of the 45 deg sweep wing undergoing the pitching motion $\alpha(t)^0 = 15 + 5 \sin(0.4t)$ at a chord Reynolds number of $R_c = 2.5 \times 10^4$ and a reduced frequency of $K = 0.5$. Both the upward and downward motions are shown side by side for the angles of attack of 10, 12, 14, 16, 18, and 20 deg. At any particular angle of attack, the flow patterns were very different during the upward and downward motions. The separation region at the downstroke was visually thicker than that at the upstroke, indicating the existence of a hysteresis loop. For a two-dimensional unsteady airfoil, the lift, drag, and moment also experience hysteresis in one oscillation cycle,[4,5] but it is caused by a convecting separation vortex rather than by the stationary separation vortices encountered in the present investigation.

When the reduced frequency is decreased to a very low value, the hysteresis should diminish and the flow should reach a quasisteady state. In the present study, the hysteresis could still be detected at K. Thus, a quasisteady state was not achieved.§

The hysteresis loop was also observed from the end view of the pitching wing obtained using a vertical sheet of light in the y-z plane at $x = 0.8c$. The dye released from the slots on the suction side of the wing marked the leading-edge separation vortex. The growth-decay of the vortex can be inferred from the size of the dye blob. The height of the dye blob, H, in several test conditions of the 45 deg sweep wing is plotted in Fig. 6. The hysteresis loop is obvious in this diagram, and several other interesting features are also revealed here. In Fig. 6a, three unsteady cases were performed at the same Reynolds number, $R_c = 5.0 \times 10^4$, but at different reduced frequencies, $K = 0.25$, 0.5, and 1.0. At an angle of attack of less than 15 deg, the values of H are not a function of the reduced frequency, and the size of the vortex in the steady case is about equal to the averaged values of H at the upstroke and downstroke. The effect of the reduced frequency becomes obvious for $\alpha > 15$ deg. At the lowest reduced frequency,

§Two-dimensional oscillating airfoil experiments indicate the presence of a hystersis loop and the lack of quasisteady behavior for reduced frequencies as low as 0.001.[14,15]

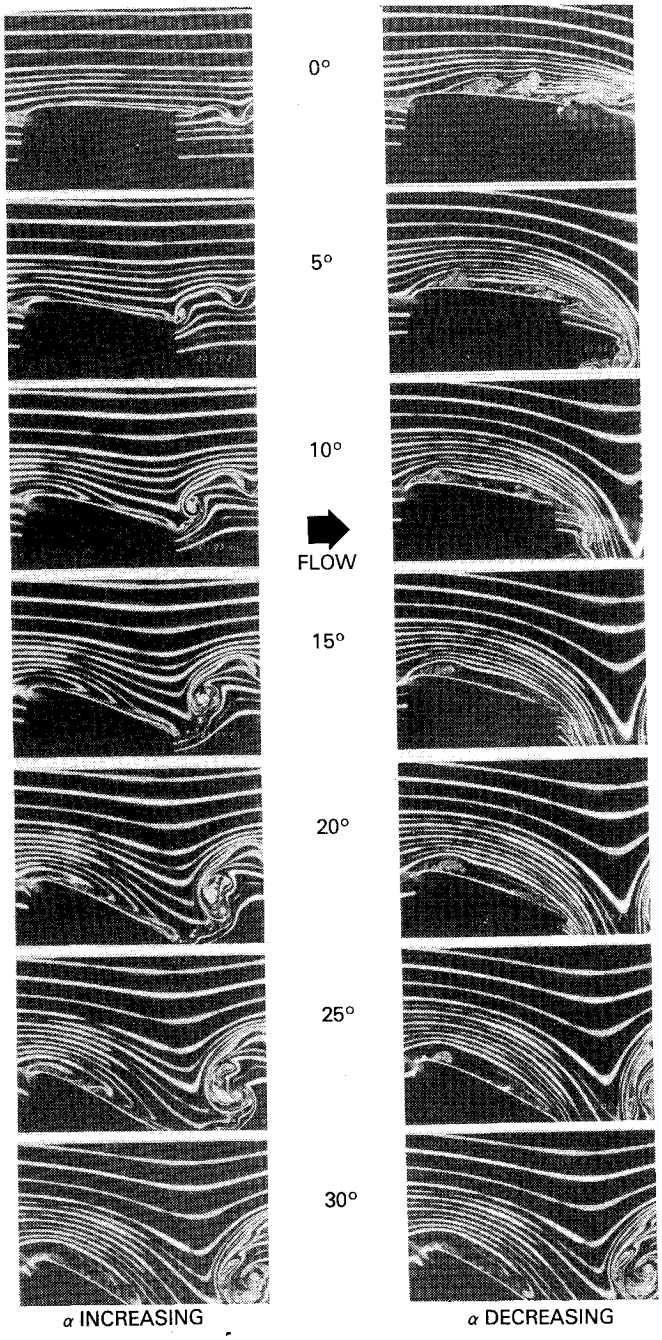

Fig. 7 Side view using the dye-layer technique. $R_c = 2.5 \times 10^4$, $K = 3.0$, $\alpha(t)^\circ = 15 + 15 \sin(2.4t)$.

$K = 0.25$, the hysteresis loop followed the trend of H in the steady case to fairly high angles of attack. At higher reduced frequencies, the deviation between the unsteady H and the static H became larger. The maximum value of H could be controlled by two time scales; the period of oscillation and a scale associated with the roll-up time of the separation vortex. At high reduced frequencies, the wing changed to a downstroke before the vortices reached the fully developed stage and, hence the maximum H decreased with increasing K. This phenomenon is due mainly to an inertial effect, and viscosity should not play a role. This is demonstrated in Fig. 6b for two unsteady cases performed at the same reduced frequency of $K = 1$, but at two different Reynolds numbers, $R_c = 2.5 \times 10^4$ and 3.4×10^5. The Reynolds numbers in these two tests were more than one order of magnitude apart; however, there is no measurable difference in the measured values of H.

Effects of the Reduced Frequency

In general, the unsteadiness on a delta wing delayed stall and prompted hysteresis, which is similar to results obtained with unsteady two-dimensional airfoils. As the oscillation frequency increased, the formation of the separation region appeared further downstream. At $K = 1$, the streamlines remained parallel to the wing surface until high angles of attack were reached.

Significant changes occurred when the reduced frequency was about π. No thick separation zone was then observed on the wing; however, a strong vortex was shed at the trailing edge as α passed through its maximum value. Figure 7 is a side view of the pitching wing visualized using the dye-layer technique. The 45-deg sweep wing underwent the pitching motion of $\alpha(t)^0 = 15 + 15 \sin(2.4t)$ at a chord Reynolds number of $R_c = 2.5 \times 10^4$ and a reduced frequency of $K = 3.0$. The movie sequence in the figure shows the wing at attack angles of 0, 5, 10, 15, 20, 25, and 30 deg during the upstroke and downstroke. The dye layers in the outer flow region indicate that the potential flow is following the motion of the wing, and that the separation region is restricted to be very close to the wing surface.

A tentative explanation for the distinct change at $K \simeq \pi$ is as follows. The reduced frequency can be viewed as the ratio of the chord to a "perturbation" wavelength: $K = \pi fc/U_\infty = \pi c/\lambda$. In other words, the perturbation wavelength is about equal to the chord length at $K = \pi$. As a matter of fact, the reattachment point can be seen near the trailing edge in Fig. 7. After the flow is reattached, a thin shear layer with intense vortices formed, and a strong vortex counterrotating with respect to the attached wing circulation was shed from the trailing edge. The induced velocity of this vortex kept the potential flow moving downward with the wing. If the perturbation wavelength was longer than the chord, i.e., $K < \pi$, the wake remained thick. The diffused vortex could not enforce a thin separation region on the wing. Based on these arguments, it appears that the Strouhal number based on the chord length is more appropriate to describe the flow than the conventional reduced frequency.

The Counterrotating Vortices

With steady flow, a detailed visualization showed that there was a small counterrotating vortex next to each primary separation vortex.[16] In the present investigation, a counterrotating vortex was also observed in ciné films of the unsteady delta wing. Moreover, this counterrotating vortex had a hysteresis loop. A pair of such vortices commonly occurred in other unsteady separated flows.[17,18] In some flows, the counterrotating vortices have a very strong dynamic influence. For example, in an impinging jet, the ring-shaped coherent structure in the shear layer induces a counterrotating vortex while it approaches the wall. The suction generated on the wall by the induced vortex was found to be considerably higher than that generated by the coherent structure.[12] The large suction associated with the counterrotating vortex implies that the aerodynamic characteristics of a given surface could be significantly altered by modifying the evolution of this vortex. This is easier than changing the flow structure far away from the wall, because an active device can be placed on the wall to alter the low-speed flow region. The importance of the counterrotating vortex on the delta wing is not clear at present. It certainly deserves further investigation, especially the counterrotating vortices located at about 60% of the semispan from the center, where the suction peaks occur.[3]

IV. Conclusions

Two delta wings with leading-edge sweeps of 45 and 60 deg were studied in a towing tank at chord Reynolds numbers up to 3.5×10^5. The wings were pitched about the quarter-chord point with sinusoidal oscillations of amplitude ± 5, ± 10, and ± 15 deg about a given mean attack angle. Food color and fluorescent dyes were used to visualize the flowfield around

the wing. Sheets of laser light excited the fluorescent dye to yield detailed flow information in the desired plane.

The three-dimensional separation process of the leading-edge vortex started from the trailing-edge corners and propagated upstream and inward. The evolution of the separation vortex revealed a hysteresis loop that is a strong function of the reduced frequency. At low reduced frequencies, the separation region on the suction side was fairly thick. A distinct change of the flow pattern happened at $K \simeq \pi$. The shedding vortex became strongly coherent in this range of reduced frequencies, and its induced velocity kept the separated region to a thin layer near the wing surface.

Acknowledgments

This work is supported by the U.S. Air Force Office of Scientific Research Contract F49620-80-C-0020, and monitored by Major M.S. Francis and Dr. J.D. Wilson. The authors would like to acknowledge the valuable help of R.F. Blackwelder, M. Cooper, and R. Srnsky.

References

[1]Jones, R.T. and Cohen, D., *High Speed Wing Theory*, Princeton University Press, Princeton, NJ, 1960.

[2]Elle, B.J., "An Investigation at Low Speed of the Flow Near the Apex of Thin Delta Wings with Sharp Leading Edges," Aeronautical Research Council, R&M 3176, Jan. 1958.

[3]Fink, P.T. and Taylor, J., "Some Early Experiments on Vortex Separation, Part II: Some Low Speed Experiments with 20 Degree Delta Wings," Aeronautical Research Council, R&M 3489, Sept. 1966.

[4]McAlister, K.W. and Carr, L.W., "Water Tunnel Visualization of Dynamic Stall," *Journal of Fluids Engineering*, Vol. 101, Sept. 1979, pp. 376-380.

[5]McCroskey, W.J., "Unsteady Airfoils," *Annual Review of Fluid Mechanics*, Vol. 14, Jan. 1982, pp. 285-311.

[6]Lambourne, N.C., Bryer, D.W., and Maybrey, J.F.M., "The Behaviour of the Leading-Edge Vortices Over a Delta Wing Following a Sudden Change of Incidence," Aeronautical Research Council, R&M 3645, March 1969.

[7]Gad-el-Hak, M., Blackwelder, R.F., and Riley, J.J., "On the Growth of Turbulent Regions in Laminar Boundary Layers," *Journal of Fluid Mechanics*, Vol. 110, Sept. 1981, pp. 73-95.

[8]Gad-el-Hak, M., Ho, C.-M., and Blackwelder, R.F., "A Visual Study of a Delta Wing in Steady and Unsteady Motion," *Unsteady Separated Flows*, edited by M.S. Francis and M.W. Luttges, University of Colorado, Colorado Springs, Aug. 1983, pp. 45-51.

[9]Gad-el-Hak, M. and Blackwelder, R.F., "The Discrete Vortices from a Delta Wing," *AIAA Journal*, Vol. 23, June 1985, pp. 961-962.

[10]Williams, J.C. III, "Incompressible Boundary-Layer Separation," *Annual Review of Fluid Mechanics*, Vol. 9, Jan. 1977, pp. 113-144.

[11]Telionis, P.P., *Unsteady Viscous Flows*, Springer-Verlag, New York, 1981.

[12]Didden, N. and Ho, C.-M., "Unsteady Separation in the Boundary Layer Produced by an Impinging Jet," *Journal of Fluid Mechanics*, in press, 1985.

[13]Ho, C.-M. and Nosseir, N.S.M., "Dynamics of an Impinging Jet. Part 1: The Feedback Mechanism," *Journal of Fluid Mechanics*, Vol. 105, April 1981, pp. 119-142.

[14]McAlister, K.W., Carr, L.W., and McCroskey, W.J., "Dynamic Stall Experiments on the NACA 0012 Airfoil," NASA TP 1100, Jan. 1978.

[15]Francis, M.S. and Keesee, J.E., "Airfoil Dynamic Stall Performance with Large Amplitude Motions," submitted to *AIAA Journal*, 1985.

[16]Fink, P.T., "Some Early Experiments on Vortex Separation, Part III: Further Experiments with 20 Degree Delta Wings," Aeronautical Research Council, R&M 3489, Sept. 1966.

[17]Freymuth, P., Bank, W., and Palmer, M., "Visualization of Accelerating Flow Around an Airfoil at High Angles of Attack," *Zeitschrift der Flugwissenschaft fuer Weltraumforschungs*, Vol. 7, July 1983, pp. 392-400.

[18]Gad-el-Hak, M. and Ho, C.-M., "Three Dimensional Effects on a Pitching Lifting Surface," AIAA Paper 85-0041, Jan. 1985.